Zinc(II)-Coordinated Oligotyrosine: A New Class of Cell Penetrating Peptide

James R. Johnson, Hua Jiang, and Bradley D. Smith*

Department of Chemistry and Biochemistry, University of Notre Dame, Notre Dame, Indiana 46556 USA. Received December 16, 2007; Revised Manuscript Received January 20, 2008

A new series of cell penetrating peptides (CPPs) are described. The peptides are oligomers of Tyr-ZnDPA, a tyrosine derivative with an appended 2,2′-dipicolylamine unit that forms a very stable coordination complex with a zinc (II) cation. This in turn allows reversible association with a chelating oxyanion such as a carboxylate or phosphate derivative. The peptide oligomers $(Tyr\text{-}ZnDPA)_n$ where $n = 1, 2, 4, 8$, are highly water soluble, but upon association with fatty acids or phospholipids they partition into an organic octanol phase. Furthermore, a fluorescent, fluorescein-labeled version of the octamer, $(Tyr\text{-}ZnDPA)_8$-Fl, can enter living mammalian cells via endocytosis and a biotin derivative can deliver fluorescein-labeled streptavidin. Fluorescence microscopy and flow cytometry experiments show that cell uptake is diminished by conditions that inhibit endocytosis. Additionally, uptake of $(Tyr\text{-}ZnDPA)_8$-Fl is greater than fluorescein labeled octaarginine (Arg_8-Fl) in all cell lines tested (CHO, COS-7, HeLa). Another difference with Arg_8-Fl is that cell uptake of $(Tyr\text{-}ZnDPA)_8$-Fl does not require the presence of heparan sulfate proteoglycans on the cell surface. This difference may eventually be of practical value because drug delivery systems that employ alternative endocytic mechanisms may be optimal for different cell lines or they may deliver selectively to different organelles within a cell.

INTRODUCTION

Spontaneous diffusion of charged or high molecular weight compounds across the cell plasma membrane is kinetically unfavored which means that many potential drugs and diagnostic reagents are ineffective because they cannot reach their intracellular targets. To overcome this transport barrier, a range of cell delivery systems have been proposed and investigated, including cell surface receptors, synthetic transporters, nanotubes, and nanoparticles (*1–4*). In the mid 1960s Ryser and Hancock discovered that cationic peptides can promote the entry of macromolecules into living cells (*5–7*), and peptide mediated delivery has subsequently been applied to a wide variety of molecular cargo (*8*). Most designs of cell penetrating peptides (CPPs) are based on a membrane translocation sequence (sometimes referred to as a protein transduction sequence) that is within the larger structure of a larger transport-active protein like HIV-Tat or the *Drosophila antennapedia* homeodomain (*9, 10*). In other cases, the peptide designs are *de novo* (*11*). Usually, CPPs enter living cells via endocytosis; however, some appear to directly translocate across the plasma membrane in an energy-independent manner (*12*). The transported cargo includes biologically active proteins, DNA, liposomes, fluorescent dyes, and nanoparticles (*13–17*), and delivery success has even been achieved in vivo (*18, 19*). Often the peptide is covalently linked to the cargo (*20*), and in some cases the linker is cleavable (*21*). There are CPPs that associate noncovalently with the cargo (*22, 23*), and also CCPs that are activated by protease cleavage of an inhibitory segment (*24*).

We have designed a novel oligomeric CPP that requires metal cations for cell delivery activity. The peptide monomer is $(Tyr\text{-}ZnDPA)_1$ a tyrosine derivative with an appended 2,2′-dipicolylamine unit that forms a stable coordination complex with a zinc (II) cation (Scheme 1) (*25*). Previously, we have shown that this water soluble, zinc-coordinated monomer can associate with a chelating oxyanion such as a carboxylate or phosphate derivative. The resulting ternary complex is net neutral and if the oxyanion is sufficiently lipophilic, it can partition from water into vesicles. Here, we describe the anion binding and membrane partitioning properties of a various oligomers of $(Tyr\text{-}ZnDPA)_n$, where $n = 1, 2, 4, 8$ (Scheme 2). These peptide oligomers are also highly water soluble, but upon association with fatty acids or phospholipids they migrate into an organic octanol phase. Furthermore, we find that fluorescently labeled versions of these peptides can enter cells via endocytosis and that a biotin derivative of these peptides can deliver fluorescently labeled streptavidin. The results of this work raise the idea of a cell delivery system that is activated by increased local concentrations of zinc (*26*), and thus may be useful for selective delivery to zinc-rich tissues or to tissues upon stimulated zinc efflux from cells (*27, 28*).

Scheme 1. Association of $(Tyr\text{-}ZnDPA)_1$ with Carboxylate

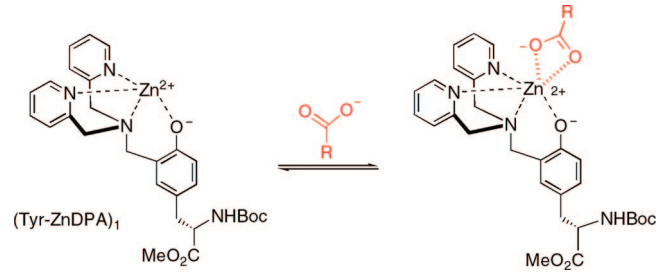

EXPERIMENTAL PROCEDURES

Synthesis. See Supporting Information.

Water/Organic Partitioning. (*1*) $(Tyr\text{-}ZnDPA)_n$ and sodium hydroxide were dissolved in water to give a 10 mM stock solution in each case. Lauric acid was dissolved in octanol to give 10 mM stock solution (*2*). To a 2 mL glass vial was added water (0.5 mL), octanol (0.5 mL), and an aqueous solution of $(Tyr\text{-}ZnDPA)_n$ (5 μL). For experiments with lauric acid, a solution of lauric acid (6 μL, 1.2 molar equiv per Zn) was added

* Fax: (+1) 574-631-6652, E-mail: smith.115@nd.edu.

10.1021/bc700466z CCC: $40.75
Published on Web 04/10/2008

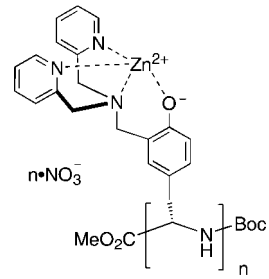

n=1, (Tyr-ZnDPA)$_1$
n=2, (Tyr-ZnDPA)$_2$
n=4, (Tyr-ZnDPA)$_4$
n=8, (Tyr-ZnDPA)$_8$

followed by a solution of sodium hydroxide (6 μL, 1.2 molar equiv). The mixed solution was shaken for 30 s and centrifuged. Spectrometric measurements were made with 100 μL aliquots from each layer. The aqueous phase was diluted with 0.1 mL octanol and 0.6 mL methanol. The octanol phase was diluted with 0.1 mL water and 0.6 mL methanol (*3*). The partitioning protocol for (Tyr-ZnDPA)$_n$-Fl is similar to above procedure. Since (Tyr-ZnDPA)$_1$-Fl is soluble in octanol rather than in water, no partition experiment was done in this case. The stock solution of (Tyr-ZnDPA)$_2$-Fl was 0.5 mM in a mixture of water and methanol (9:1). The stock solutions of (Tyr-ZnDPA)$_4$-Fl and (Tyr-ZnDPA)$_8$-Fl were 1 mM in water.

Eukaryotic Cell Culture. CHO, PGSA, PGSD, COS-7, and HeLa cells were cultured according to ATCC protocols. All cell lines were cultured in T75 cell culture flasks with vented caps and incubated at 37 °C in a humidified 5% CO_2 atmosphere. For fluorescence microscopy, cells were plated out on 8-well microscope chambered slides and allowed to grow to approximately 80% confluence. Upon treatment and incubation with CPPs, cells were rinsed 3 times with phenol free Dublecco's Minimum Essential Medium (DMEM) containing 2 mM L-glutamine, glucose, and supplemented with 10% fetal bovine serum. For flow cytometry all cell cultures were grown in 6-well cell culture plates to approximately 80% confluence. In preparation for flow cytometry cells were rinsed with phosphate buffered saline solution and then trypsinized for 10 min to remove externally bound peptide and to detach cells from the surface of well plates. Upon trypsinization, cells were resuspended in phenol-free DMEM. For both flow cytometry and fluorescence microscopy cells were analyzed in phenol-free DMEM.

Cell Toxicity. Cell toxicity was assessed via MTT assay using the Vybrant MTT Cell Proliferation Assay Kit (Invitrogen, V-13154). A 200 μL mixture of cells (approximately 5×10^4 cells/mL) in growth media were dispensed into each well of a 96-well plate and allowed to grow to 80% confluence. An aliquot of 1 mM (Tyr-ZnDPA)$_8$ in 50:50 water/methanol was administered to the first well in each treatment and subsequent wells were given a serial 2-fold dilution. The cells were allowed to incubate for 6 h at 37 °C, then the growth medium was removed and replaced with 100 μL of growth media supplemented with [3-(4,5-dimethylthiazol-2-yl)-2,5-diphenyltetrazolium bromide] (MTT) at a concentration of 1.2 mM. The cells were incubated at 37 °C for 4 h then treated with 100 μL of an SDS-HCl solution to kill the cells, and dissolve the formazan product. The SDS-HCl solution was prepared by adding 10 mL of 0.01 M HCl to 1 g of SDS. The SDS-HCl/cell solution was then incubated for 12 h at 37 °C, after which the absorbance of each well was read at 570 nm. In order to determine the viability in each sample the following equation was used:

$$\text{Cell Viability} = (\text{Abs} - \text{Abs}_{\text{Neg}})/(\text{Abs}_{\text{Con}} - \text{Abs}_{\text{Neg}})$$

where Abs is the absorbance of the test well, Abs_{Neg} is the absorbance of the negative control (no cells added to the well)

Scheme 2. Schematic View of (Tyr-ZnDPA)$_n$ and Association with Carboxylates

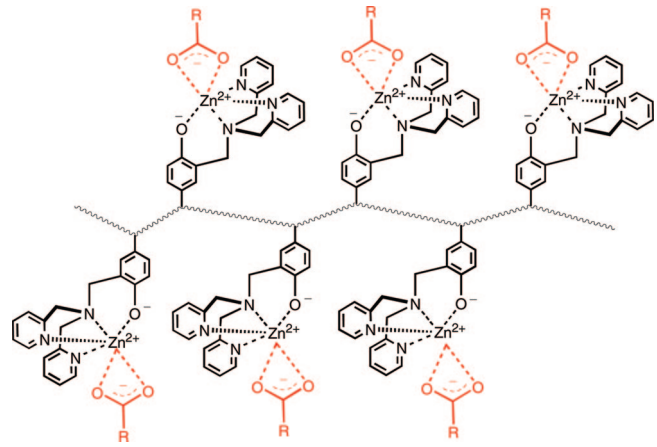

and Abs_{Con} is the absorbance of wells in which cells were not treated with (Tyr-ZnDPA)$_8$.

Fluorescence Microscopy. Fluorescence microscopy was conducted on a Nikon Eclipse TE-2000 U epifluorescence microscope equipped with blue field (Exciter: D360/40×, Dichroic: 400DCLP, Emitter: 460/50m), green field (Exciter: D360/40×, Dichroic: 400DCLP, Emitter: HQ535/50m), red field (Exciter: HQ545/30×, Dichroic: Q570LP, Emitter: HQ610/75m) filters, and far red (Exciter: HQ620/60X, Dichroic: 660LP, Emitter: HQ700/75m) filters. Images were acquired using a Photometrics 512-B black and white digital camera and appropriate field colors were added using Metamorph Software V6.2.

Flow Cytometry. Flow cytometry was conducted on a Beckman Coulter MPL 500 flow cytometer, and data was manipulated using the instrument's MPL and CXP software packages. After incubation, the cell cultures were prepared for flow cytometry analysis by removing the cell growth media, rinsing with PBS buffer, and treating with trypsin. This served to detach the cells from the culture wells and to degrade any remaining fluorescent peptide on the outside of the cells. Cell populations that were not pretreated in this manner exhibited greater fluorescence intensity due to externally bound peptide. Analysis was conducted for a minimum of 10 000 counting events.

Endocytosis Inhibition. For inhibition of endocytosis, cells were incubated at 4 °C for 15 min, treated with 10 μM (Tyr-ZnDPA)$_8$-Fl in growth media, and incubated for another 3 h at 4 °C. Cells were then prepared for analysis as previously described. For ATP depletion, cells were prenincubated in growth media supplemented with 0.1% NaN_3 and 50 mM deoxyglucose for 1 h, then treated with 10 μM (Tyr-ZnDPA)$_8$-Fl and incubated for 3 h. For specific endocytosis mechanisms, cells were treated with chlorpromazine (30 μM), 400 mM sucrose, nystatin (25 μg/mL), amiloride (3 mM), or wortmannin (10 μM) for 1 h prior to administration of (Tyr-ZnDPA)$_8$-Fl in growth media. After a 3 h incubation, cells were prepared for flow cytometry analysis.

RESULTS

Synthesis. The doubly protected amino acid (Tyr-DPA)$_1$ was prepared in one step and large scale using cheap starting materials. The oligomeric series (Tyr-DPA)$_n$, where $n = 1, 2, 4, 8$ was subsequently constructed in high yields (≥80% for each step) using solution-state amide coupling chemistry with EDC/HOBt as the activating agent. Chromatographic purification was greatly facilitated by using silica gel and an admixture of acetonitrile/ammonium hydroxide as the eluent. The pure

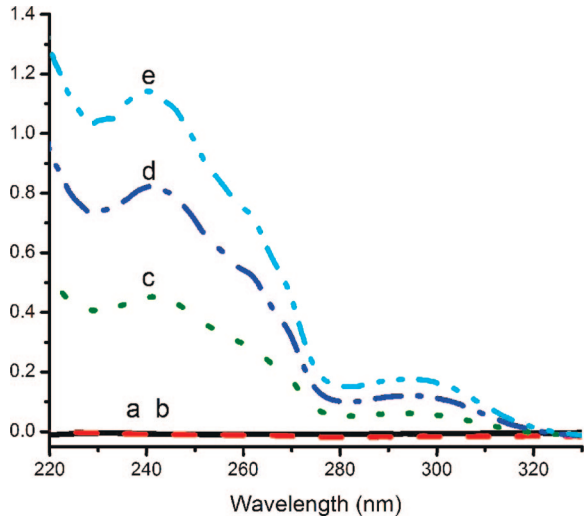

Figure 1. Absorption spectra of octanol phase after partitioning of (Tyr-ZnDPA)$_8$ (10 μM) between water and octanol with various molar equivalents of sodium laurate per Zn(II); (a) 0 equiv, (b) 0.5 equiv, (c) 0.75 equiv, (d) 1 equiv, (e) 1.5 equiv.

(Tyr-DPA)$_n$ peptides were converted into zinc(II) complexes, (Tyr-ZnDPA)$_n$, by simply stirring with a stoichiometric amount of $Zn(NO_3)_2$. To make the fluorescent conjugates, (Tyr-ZnDPA)$_n$-Fl, the amine versions of (Tyr-DPA)$_n$ were linked to FITC via an aminohexanioic acid chain, and the pure peptides converted into zinc(II) complexes. Fluorescein labeled octa(arginine), (Arg$_8$-Fl) was prepared by reported methods (*29*).

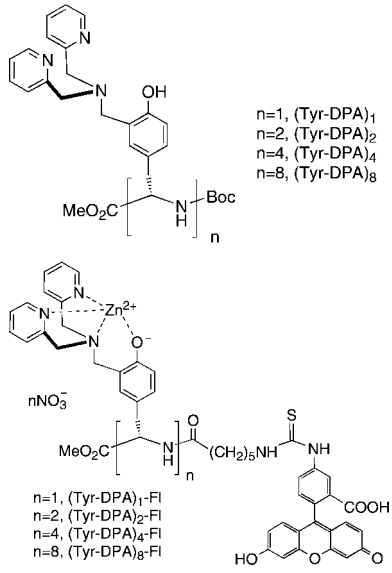

Liquid Water/Organic Partitioning Studies. The partitioning of unlabeled peptides (Tyr-ZnDPA)$_n$ between water and octanol is easily monitored by the UV absorption of the aromatic groups at 240 and 300 nm. In all cases, the zinc-coordinated oligomers are highly water-soluble and they reside completely in the aqueous phase. However, the presence of sodium laurate ($\geq$1.5 mol equiv per zinc cation) induces complete migration of each oligomer into the octanol phase. As shown in Figure 1, the presence of 0.5 mol equiv of sodium laurate is able to move significant amounts of the longest oligomer, (Tyr-ZnDPA)$_8$ into the octanol, but complete partitioning requires 1.5 mol equiv of laurate.

Similar phase transfer results were obtained with the fluorescein conjugated oligomers (Tyr-ZnDPA)$_n$-Fl. In this case, the yellow color of fluorescein tag can be monitored by the naked eye, and as shown in Figure 2, the sodium laurate promotes complete partitioning of (Tyr-ZnDPA)$_8$-Fl into the octanol layer. In Figure 3 is a comparison of the (Tyr-ZnDPA)$_8$-Fl partitioning induced by sodium laurate and the anionic phospholipid 1-palmitoyl-2-oleoylphosphatidylglycerol (POPG). In both cases, there is extensive peptide migration into the organic phase but the process is achieved more slightly readily with the POPG, reflecting its comparatively greater lipophilicity and higher affinity for the zinc cations in the peptide. The same (Tyr-ZnDPA)$_8$-Fl partitioning results were obtained with the anionic phospholipids 1-palmitoyl-2-oleoylphosphatidic acid (POPA) and 1-palmitoyl-2-oleoylphosphatidylserine (POPS), whereas no partitioning into the organic layer was induced by the presence of POPC (see Supporting Information).

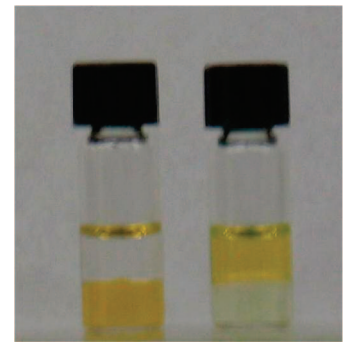

Figure 2. Partitioning of (Tyr-ZnDPA)$_8$-Fl (1 μM) between water and octanol: (left) with no sodium laurate present the peptide is completely in the lower aqueous phase. (right) the presence of 1.5 mol equiv of sodium laurate per Zn(II) induces complete migration into the upper octanol phase.

Octanol partitioning was also used to evaluate the affinity of (Tyr-ZnDPA)$_8$-Fl for the multianionic polysaccharide heparin (sodium salt from porcine intestinal mucosa, average molecular weight 3000 g/mol). In this case, the heparin was used as a water-soluble inhibitor of laurate induced transfer of (Tyr-ZnDPA)$_8$-Fl into the organic phase. As shown in Figure 4, peptide partitioning into octanol was prevented when the level of heparin in the aqueous phase was above 60 μg/mL. We infer that the multianionic heparin has a strong affinity for (Tyr-ZnDPA)$_8$-Fl and the ternary complex is not lipophilic.

Penetration of Fluorescent (Tyr-ZnDPA)$_n$ into Living Cells. The fluorescent peptides (Tyr-ZnDPA)$_n$-Fl were administered to a variety of eukaryotic mammalian cell lines (CHO, COS-7, HeLa) and examined for cellular uptake using fluorescence microscopy. Figure 5 shows fluorescent micrographs of CHO and COS-7 cells that have been incubated with (Tyr-ZnDPA)$_8$-Fl (10 μM) in serum supplemented growth media for 3 h at 37 °C. Binding of the (Tyr-ZnDPA)$_8$-Fl to the exterior of the cell was observed as early as 15 min after treatment and likely occurs immediately after administration of the compound to the cell culture. Within 1 h the fluorescence was confined to punctuate compartments within the cell. The presence of serum or growth media did not appear to inhibit uptake; however, administration of these peptides to cells in phosphate buffered saline caused precipitation, and diminished cell uptake as judged by fewer fluorescent endosomal compartments.

The amount of cell uptake of (Tyr-ZnDPA)$_n$-Fl was quantified by flow cytometry. The flow cytometry histograms in Figure 6 show that the order of uptake in HeLa cells is (Tyr-ZnDPA)$_8$-Fl > (Tyr-ZnDPA)$_4$-Fl > (Tyr-ZnDPA)$_2$-Fl. No uptake or cell surface binding was observed with (Tyr-ZnDPA)$_1$-Fl. Thus, cell adhesion and uptake increases substantially with the length and multivalency of the peptide. The uptake of (Tyr-ZnDPA)$_8$-Fl and Arg$_8$-Fl in different cell lines was compared by flow cytometry (see Supporting Information). With HeLa cells the

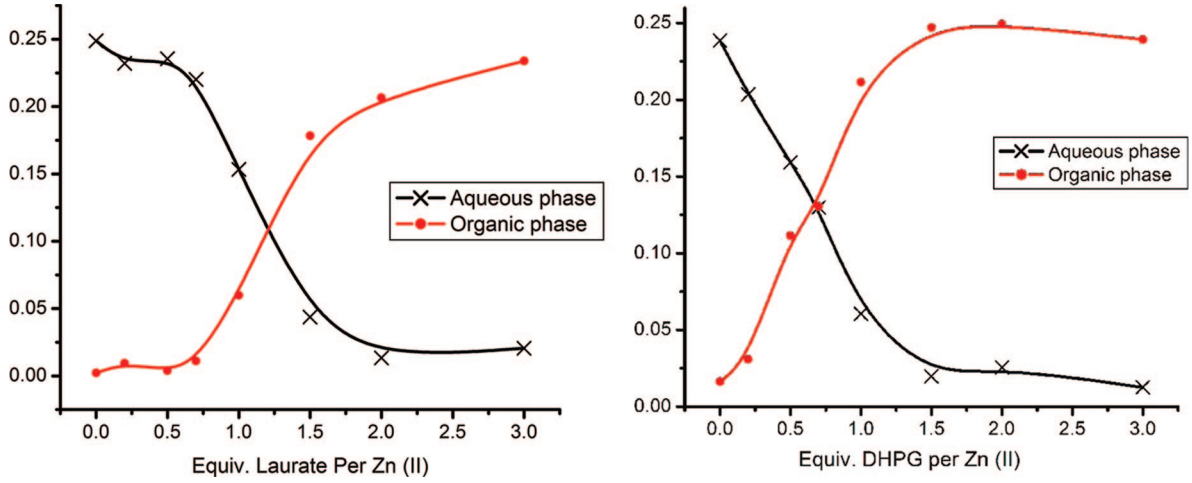

Figure 3. Amount of (Tyr-ZnDPA)$_8$-Fl (1 μM) (reflected by absorbance at 500 nm) in aqueous and organic phase after partitioning between water and octanol in the presence of: (left) various molar equivalents of sodium laurate per Zn(II); (right) various molar equivalents of POPG per Zn(II).

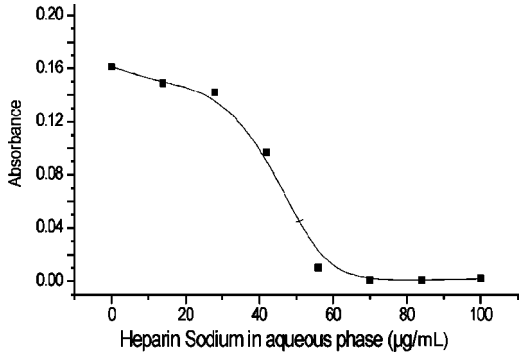

Figure 4. Amount of (Tyr-ZnDPA)$_8$-Fl (1 μM) in the organic phase (reflected by absorbance at 500 nm) for a two phase aqueous/octanol mixture that also contains sodium laurate (two molar equivalents of per Zn(II)) and various amounts of heparin sodium in the aqueous phase.

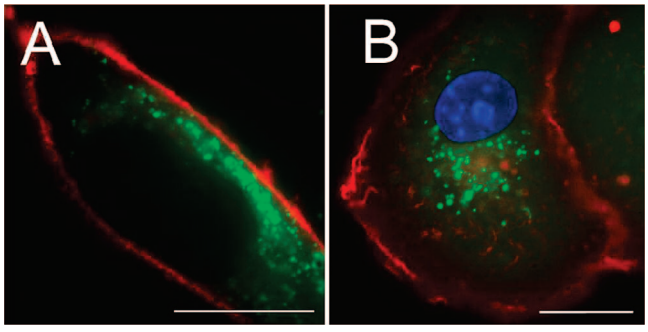

Figure 5. Panel A, a single CHO cell showing uptake of (Tyr-ZnDPA)$_8$-Fl (green). The plasma membrane is costained with FM 4–64 (1 μM) (red). Panel B, a single COS-7 cell showing uptake of (Tyr-ZnDPA)$_8$-Fl (10 μM) (green). The cellular membranes are costained with FM 4–64 (1 μM) (red) and the nucleus is costained with Hochest 33342 (1 μM) (blue). The bars denote a distance of 20 μm.

uptake of (Tyr-ZnDPA)$_8$-Fl was slightly greater, but with CHO and COS-7 cells the uptake was quite superior.

The toxicity of (Tyr-ZnDPA)$_8$ was determined by measuring cell viability using a standard MTT assay. The viability of CHO cells was unaffected by (Tyr-ZnDPA)$_8$ concentrations up to 40 μM, whereas the COS-7 cells were slightly effected with an approximate LD_{50} of 60 μM. With both cell lines there was little, if any measurable toxicity at the concentrations used in this study (10 μM).

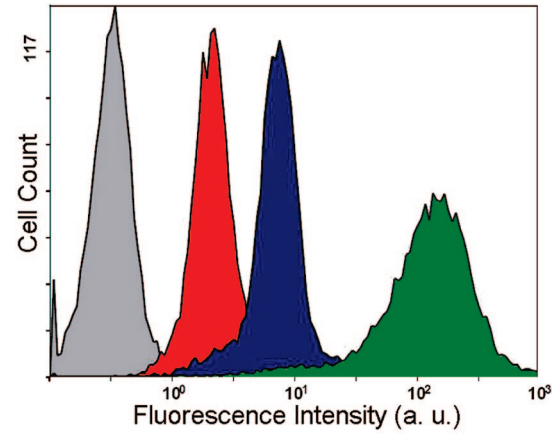

Figure 6. Overlay of flow cytometry histograms showing cellular uptake of the zinc tyrosine oligomers (10 μM) in HeLa cells. Histograms are as follows: gray, untreated cells; red, cells treated with of (Tyr-ZnDPA)$_2$-Fl; blue, cells treated with (Tyr-ZnDPA)$_4$-Fl; green, cells treated with (Tyr-ZnDPA)$_8$-Fl.

Table 1. Percent Cellular Uptake of (Tyr-ZnDPA)$_8$-Fl in the Presence of a Given Inhibitor As Quantified by Flow Cytometry[a]

		cell line		
compound	inhibits	COS-7	CHO	HeLa
4 °C incubation	endocytosis	0	0	0
NaN_3/DOG	endocytosis	0	0	0
Chlorpromazine	endocytosis[b]	6	13	50
Sucrose	endocytosis[b]	6	13	2
Nystatin	endocytosis[c]	60	40	80
Amiloride	pinocytosis	100	100	100
Wortmannin	pinocytosis	100	100	100

[a] Values are compared to uptake in the absence of inhibitor. [b] Clathrin-mediated endocytosis. [c] Caveolin-mediated endocytosis.

To determine how much of the cell uptake was due to endocytosis, the cell incubations were repeated under various conditions that inhibit endocytic processes (Table 1). The first method involved incubation of cell cultures at low temperature. Fluorescence microscopy and flow cytometry showed that incubation at 4 °C greatly inhibited the uptake of (Tyr-ZnDPA)$_8$-Fl. In addition, there was no entry into cells whose ATP levels were depleted of by preincubation with growth media supplemented with 0.1% NaN_3 and 50 mM deoxyglucose (DOG). These results indicate that cellular uptake occurs via one or more endocytosis mechanisms.

Table 2. Percent Uptake of Arg_8-Fl and $(Tyr\text{-}ZnDPA)_8$-Fl into PGSA and PGSD Cells Compared to Uptake into CHO Cells

peptide (10 μM)	PGSA	PGSD	CHO
Arg_8-Fl	<5	90	100
$(Tyr\text{-}ZnDPA)_8$-Fl	100	160	100

Additional mechanistic insight was gained by treating the cells with compounds that inhibit specific endocytosis processes. Separate samples of cells were each pretreated with an inhibitor prior to addition of $(Tyr\text{-}ZnDPA)_8$-Fl. Chlorpromazine and sucrose are known to be inhibitors of clathrin-mediated endocytosis while nystatin inhibits caveolin-mediated mechanisms (*30*). Cells were also treated with amiloride and wortmannin which inhibit pinocytosis. The amount of cell uptake was determined using flow cytometry and as summarized in Table 1, the inhibition varied with cell-type. The most effective inhibitors were chloropromazine and sucrose; whereas, amiloride and wortmannin were ineffective. Taken together the data in Table 1 indicates that $(Tyr\text{-}ZnDPA)_8$-Fl enters cells primarily by clathrin-mediated endocytosis.

There is strong evidence that oligo(arginine) internalization requires the presence of cell surface heparan sulfate proteoglycans (*30*). Since the phase transfer studies demonstrated that $(Tyr\text{-}ZnDPA)_8$-Fl also associates with the heavily sulfonated, heparin, we investigated if cell internalization was mediated by heparan sulfate proteoglycans. Our study compared the uptake into native CHO cells with entry into cells that were deficient in certain types of proteoglycans; that is, the PGSA 745 and PGSD 677 strains of CHO cells. PGSA cells do not have glycosaminoglycans because they are deficient in xylosyltransferase, which catalyzes attachment of the first sugar in glycosaminoglycan synthesis. Similarly, PGSD cells are deficient in both N-acetylglucosaminyltransferase and glucuronyltransferase activities and do not produce heparan sulfate, but they do produce chondroitin sulfate (*31, 32*). Separate samples of each cell type were treated with Arg_8-Fl and $(Tyr\text{-}ZnDPA)_8$-Fl (10 μM) and analyzed by both fluorescence microscopy and flow cytometry (Table 2). The decreased uptake of Arg_8-Fl was consistent with literature expectations. In contrast, the uptake of $(Tyr\text{-}ZnDPA)_8$-Fl into PGSA and PGSD cells was the same as native CHO cells (see Supporting Information). It appears that the presence of heparan sulfate proteoglycans on the cell surface is not necessary for uptake of $(Tyr\text{-}ZnDPA)_8$-Fl.

Streptavidin Delivery into Living Cells. Delivery of the versatile and multivalent protein, streptavidin into living cells is an important technical goal because it can be used to cotransport biotinylated cargo or target biotinylated intracellular targets. Previous studies have used Tat-streptavidin fusion protein (*33*), biotinylated antibody (*34*), biotinylated steroid (*35*), and biotinylated carbon nanotube (*36*). We prepared some zinc tyrosine-biotin conjugates and evaluate their abilities to noncovalently bind and transport the tetrameric streptavidin (molecular weight 64 kD) into living cells. Two groups of peptide-biotin conjugates were prepared. Direct attachment of the biotin to the N-terminal of the zinc tyrosine oligomers gave the series $(Tyr\text{-}ZnDPA)_n$-Biotin, whereas a longer spacer was attached to the C-terminal to make the series, $(Tyr\text{-}ZnDPA)_n$-TEO-Biotin.

These biotin conjugates were mixed separately with FITC labeled streptavidin and administered to living cells. There was no uptake of FITC-streptavidin when it was mixed with the $(Tyr\text{-}ZnDPA)_n$-Biotin, but cell delivery was achieved when the FITC-streptavidin was mixed with $(Tyr\text{-}ZnDPA)_n$-TEO-Biotin. Typical results with $(Tyr\text{-}ZnDPA)_8$-TEO-Biotin are shown in Figure 7. The fluorescence emission of the transported FITC-streptavidin appeared in the same types of endosomal compartments as the $(Tyr\text{-}ZnDPA)_n$-Fl series. A stoichiometry study indicated that FITC-streptavidin uptake increased until the $(Tyr\text{-}ZnDPA)_8$-TEO-Biotin: FITC-streptavidin ratio reached 4:1 and then remained constant for higher values.

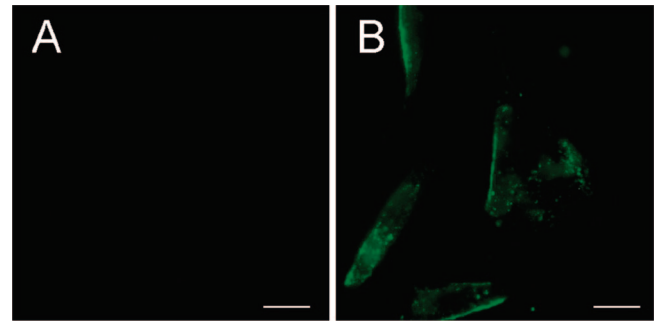

Figure 7. Fluorescence microscopy images of COS-7 cells treated with FITC-streptavidin (panel A) or $(Tyr\text{-}ZnDPA)_8$-TEO-Biotin complexed with FITC-streptavidin (panel B). The complexes were formed prior to cell treatment and complexes were administered at a concentration of 250 nM streptavidin.

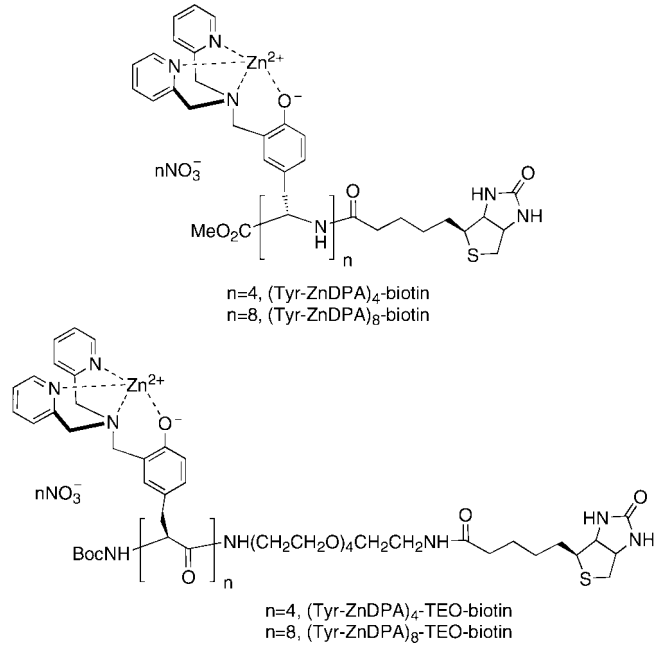

DISCUSSION

Cellular uptake of the $(Tyr\text{-}ZnDPA)_n$ peptides into living cells increases with peptide length and higher order multivalency. The biotin conjugate $(Tyr\text{-}ZnDPA)_8$-TEO-Biotin is able to promote internalization of the fluorescently labeled protein, streptavdin. In contrast, the biotin conjugate $(Tyr\text{-}ZnDPA)_8$-Biotin with a shorter linker is ineffective. The shorter linker may not allow the biotin group to reach the binding pocket of the streptavidin, or alternatively, the large streptavidin protein may prevent the peptide from achieving favorable interactions with the cell surface target (*37*). In any case, linker length is important for effective streptavidin delivery.

Uptake of the fluorescent octamer $(Tyr\text{-}ZnDPA)_8$-Fl is greater than the analogous Arg_8-Fl in all cell lines tested. Another striking difference with Arg_8-Fl is that cell uptake of $(Tyr\text{-}ZnDPA)_8$-Fl does not require the presence of heparan sulfate proteoglycans on the cell surface. It appears that the $(Tyr\text{-}ZnDPA)_n$ peptides target other markers on the cell surface, perhaps anionic phospholipids, negatively charged proteins (*38*), or cell surface carbohydrates (*39*). Our water/organic partitioning studies show that the $(Tyr\text{-}ZnDPA)_n$ peptides associate with anionic phospholipids and fatty acids to form lipophilic complexes that partition into organic phases. However, the cell entry

mechanism is primarily clathrin-mediated endocytosis and not passive diffusion through the plasma membrane. It appears that the $(Tyr\text{-}ZnDPA)_n$ peptides bind to the membrane surface and trigger an endocytosis event (*40*), or they may internalized by the routine membrane recycling mechanisms of the cell (*41–43*). While further studies are needed to fully elucidate the uptake mechanism(s) used by the $(Tyr\text{-}ZnDPA)_n$ peptides, the data in hand suggest that it differs to oligo(arginine) internalization. The distinction may eventually be of practical value because drug delivery systems that employ alternative endocytic mechanisms may be optimal for different cell lines or they may deliver selectively to different organelles within a cell (*44–46*).

The fluorescence microscopy data indicate that the transported peptides (or cotransported streptavidin) remain localized within endosomal compartments of the living cells. Therefore to effectively reach the cell cytosol it will be necessary to trigger endosomal release using an adjuvant (*47, 48*). We plan to determine if these multivalent $(Tyr\text{-}ZnDPA)_n$ peptides can form noncovalent complexes with anionic cargo such as oligonucleotides and deliver them into cells. Another idea is to conjugate a $(Tyr\text{-}ZnDPA)_n$ peptide to a hydrophobic tryptophan-rich sequence and produce a zinc-dependent mimic of the noncovalent protein carrier Pep-1 (*49*). It may even be possible to create triggered cell delivery devices that can be activated by increases in local concentrations of zinc (II) cation.

ACKNOWLEDGMENT

This work was supported by the NIH and the Notre Dame CEST. We warmly thank Dr. W. Matthew Leevy for advice and assistance.

Supporting Information Available: Synthetic procedures and flow cytometry histograms. This material is available free of charge via the Internet at http://pubs.acs.org.

LITERATURE CITED

(1) Dunehoo, A. L., Anderson, M., Sumit, M., Kobayashi, N., Berkland, C., and Siahaan, T. J. (2006) Cell adhesion molecules for targeted drug delivery. *J. Pharm. Sci. 95*, 1856–1871.

(2) Janot, V., and Regen, S. L. (2005) A needle-and-thread approach to bilayer transport: Permeation of a molecular umbrella-oligonucleotide conjugate across a phospholipid membrane. *J. Am. Chem. Soc. 127*, 22–23.

(3) Kam, N. W., Jessop, T. W., Wender, P. A., and Dai, H. (2004) Nanotube molecular transporters: Internalization of carbon nanotube-protein conjugates into mammalian cells. *J. Am. Chem. Soc. 126*, 6850–6851.

(4) Kohane, D. S. (2007) Microparticles and nanoparticles for drug delivery. *Biotechnol. Bioeng. 96*, 203–209.

(5) Ryser, H. J., and Hancock, R. (1965) Histones and basic polyamino acids stimulate the uptake of albumin by tumor cells in culture. *Science 150*, 501–503.

(6) Ryser, H. J. (1967) Uptake of protein by mammalian cells: an underdeveloped area. The penetration of foreign proteins into mammalian cells can be measured and their functions explored. *Science 159*, 390–396.

(7) Ryser, H. J. (1968) A membrane effect of basic polymers dependent on molecular size. *Nature 215*, 934–936.

(8) Wigstaff, K. M., and Jans, D. A. (2006) Protein transduction: Cell penetrating peptides and their therapeutic applications. *Curr. Med. Chem. 13*, 1371–1387.

(9) Torchilin, V. P., Levchenko, T. S., Rammohan, R., Volodina, N., Papahadjopoulos-Sternberg, G., and D'Souza, G. G. (2003) Cell transfection *in vitro* and *in vivo* with nontoxic tat peptide-liposome-DNA complexes. *Proc. Natl. Acad. Sci. U.S.A. 100*, 1972–1977.

(10) Pietersz, G. A., Li, W., and Apostolopoulos, V. (2001) A 16-mer peptide (RQIKIWFQNRRMKWKK) from Antennapedia preferentially targets the Class I pathway. *Vaccine 9*, 1397–405.

(11) Temsamani, J., and Vidal, P. (2004) The use of cell-penetrating peptides for drug delivery. *Drug Discovery Today 9*, 1012–1019.

(12) Futaki, S. (2002) Arginine-rich peptides: Potential for intracellular delivery of macromolecule and the mystery of the translocation mechanism. *Int. J. Pharm. 245*, 1–7.

(13) Lu, J., Higashimoto, Y., Appella, E., and Celis, E. (2004) Multiepitope trojan antigen peptide vaccines for the induction of antitumor CTL and Th immune responses. *J. Immunol. 172*, 4575–4582.

(14) Rudolph, C., Plank, C., Lausier, J., Schillinger, U., Muller, R. H., and Rosenecker, J. (2003) Oligomers of the Arginine-rich Motif of the HIV-1 TAT protein are capable of transferring plasmid DNA into cells. *J. Biol. Chem. 278*, 11411–11418.

(15) Torchilin, V. P., Rammohan, R., Wiessig, V., and Levachenko, T. S. (2001) Tat peptide on the surface of liposomes affords their efficient intracellular delivery even at low temperature and in the presence of metabolic inhibitors. *Proc. Natl. Acad. Sci. U.S.A. 98*, 8786–8791.

(16) Bullok, K. E., Gammon, S. T., Violini, S., Prantner, A. M., Villalobos, V. M., Sharma, V., and Piwnica-Worms, D. (2006) Permeation peptide conjugates for in vivo molecular imaging applications. *Mol. Imag. 5*, 1–15.

(17) Josephson, L., Tung, C. H., Moore, A., and Weisselader, R. (2004) High-efficiency intracellular magnetic labeling with novel superparamagnetic-Tat peptide conjugates. *Bioconjugate Chem. 10*, 186–191.

(18) Mi, Z., Mai, J., Lu, X., and Robbins, P. D. (2000) Characterization of a class of cationic peptides able to facilitate efficient protein transduction *in Vitro* and *in Vivo*. *J. Mol. Therapy 2*, 339–347.

(19) Schwarze, S. R., Ho, A., Vocero-Akbani, A., and Dowdy, S. F. (1999) In vivo protein transduction: Delivery of a biologically active protein into the mouse. *Science 285*, 1569–1572.

(20) Venkatesan, N., and Kim, B. H. (2006) Peptide conjugates of oligonucleotides: Synthesis and applications. *Chem. Rev. 106*, 3712–3761.

(21) Vocero-Akani, A., Heyden, N., Lissy, N., Ratner, L., and Dowdy, R. (1999) S. Killing HIV-infected cells by transduction with an HIV protease activated caspase-3 protein. *Nat. Med. 5*, 29–33.

(22) Gros, E., Deshayes, S., Morris, M. C., Aldrian-Herrada, G., Depollier, J., Heitz, F., and Divita, G. (2006) A non-covalent peptide-based strategy for protein and peptide nucleic acid transduction. *Biochim. Biophys. Acta - Biomembranes 1758*, 384–393.

(23) Myrberg, H., Lindgren, M., and Langel, U. (2007) Protein delivery by the cell-penetrating peptide YTA2. *Bioconjugate Chem. 18*, 170–174.

(24) Jiang, T., Olson, E. S., Nguyen, Q. T., Roy, M., Jennings, P. A., and Tsien, R. Y. (2004) Tumor imaging by means of proteolytic activation of cell-penetrating peptides. *Proc. Natl. Acad. Sci. U.S.A. 101*, 17867–17872.

(25) Jiang, H., O'Neil, E. J., DiVittorio, K. M., and Smith, B. D. (2005) Anion-mediated phase transfer of Zinc(II)-coordinated tyrosine derivitives. *Org. Lett. 7*, 3013–3017.

(26) Füssl, A., Schleinfenbaum, A., Göritz, M., Riddell, A., Schultz, C., and Krämer, R. (2006) Cellular uptake of PNA-terpyridine conjugates and its enhancement by Zn^{2+} ions. *J. Am. Chem. Soc. 128*, 5986–5987.

(27) Qian, W., Gee, K. R., and Kennedy, R. (2003) Imaging of Zn^{2+} release from pancreatic beta-cells at the level of single excytotic events. *Anal. Chem. 75*, 3468–3475.

(28) Liuzzi, J. P., and Cousins, R. J. (2004) Mammalian zinc transporters. *Annu. Rev. Nutr.* 24151–24172.

(29) Wender, P. A., Rothbard, J. B., Jessop, T. C., Kreider, E. L., and Wylie, B. L. (2004) Oligocarbamate molecular transporters: Design, synthesis, and biological evaluaion of a new class of transporters for drug delivery. *J. Am. Chem. Soc. 124*, 13382–13383.

(30) Richard, J. P., Melikov, K., Brooks, H., Prevot, P., Lebleu, B., and Chernomordik, L. P. (2005) Cellular uptake of unconjugated TAT peptide involves clathrin-dependent endocytosis and heparan sulfate receptors. *J. Biol. Chem. 280*, 15300–15306.

(31) Esko, J. D., Stewart, T. E., and Taylor, W. H. (1985) Animal cell mutants defective in glycosaminoglycan biosynthesis. *Proc. Natl. Acad. Sci. U.S.A. 82*, 3197–3201.

(32) Esko, J. D., Rostand, K. S., and Weinke, J. L. (1988) Tumor formation dependent on proteoglycan biosynthesis. *Science 241*, 1092–1096.

(33) Albarran, B., To, R., and Stayton, P. R. (2005) A Tat-streptavidin fusion protein directs uptake of biotinylated cargo into mammalian cells. *Protein Eng. Des. Sel. 18*, 147–152.

(34) Lackey, C. A., Press, O. W., Hoffman, A. S., and Stayton, P. S. (2002) A biomimetic pH-responsive polymer directs endosomal release and intracellular delivery of an endocytosed antibody complex. *Bioconjugate Chem. 13*, 996–1001.

(35) Hussey, S. L., and Peterson, B. S. (2002) Efficient delivery of streptavidin to mammalian cells: Clathrin-mediated endocytosis regulated by a synthetic ligand. *J. Am. Chem. Soc. 124*, 6265–6273.

(36) Kam, N. W., Jessop, T. C., Wender, P. A., and Dai, H. (2004) Nanotube molecular transporters: Internalization of carbon nanotube-protein conjugates into mammalian cells. *J. Am. Chem. Soc. 126*, 6850–6851.

(37) Hussey, S. L., and Peterson, B. R. (2002) Efficient delivery of streptavidin to mammalian cells: Clathrin-mediated endocytosis regulated by a synthetic ligand. *J. Am. Chem. Soc. 124*, 6265–6273.

(38) Nisole, S., Krust, B., Callebaut, C., Guichard, G., Muller, S., Briand, J. P., and Hovanessian, A. G. (1999) The anti-HIV pseudopeptide HB-19 forms a complex with the cell-surface-expressed nucleolin independent of heparan sulfate proteoglycans. *J. Biol. Chem. 274*, 27875–27884.

(39) Fukuda, M. (1994) Cell surface carbohydrates: Cell-type specific expression. *Molecular Glycobiology* (Fukuda, M. and Hindsgaul, O. Eds.) pp. 1–52, Oxford University Press, New York.

(40) Fischer, P. M. (2007) Cellular uptake mechanisms and potential therapeutic utility of peptidic cell delivery vectors: Progress 2001−2006. *Med. Res. Rev. 27*, 755–795.

(41) Brooks, H., Lebleu, B., and Vives, E. (2005) Tat peptide-mediated cellular Delivery: Back to basics. *Adv. Drug Delivery Rev. 57*, 559–577.

(42) Kilic, G., Doctor, R. B., and Fitz, J. G. (2001) Insulin stimulates membrane conductance in a liver cell line: Evidence for insertion of ion channels through a phosphoinositide 3-kinase-dependent mechanism. *J. Biol. Chem. 276*, 26762–26768.

(43) Neuhaus, E. M., and Soldati, T. (2000) A myosin I is involved in membrane recycling from early endosomes. *J. Cell Biol. 150*, 1013–1026.

(44) Bareford, L. M., and Swaan, P. W. (2007) Endocytic mechanisms for targeted drug delivery. *Adv. Drug Delivery Rev. 59*, 748–758.

(45) Medina-Kauwe, L. K. (2007) Alternative endocytic mechanism exploited by pathogens: New avenues for therapeutic delivery? *Adv. Drug Delvery Rev. 59*, 798–809.

(46) Tarrago-Trani, M. T., and Storrie, B. (2007) Alternative routes for drug delivery to the cell interior: Pathways to the Golgi apparatus and endoplasmic reticulum. *Adv. Drug Delivery Rev. 59*, 782–797.

(47) Vogel, K., Wang, S., Lee, R. J., Chmielewski, J., and Low, P. S. (1996) Peptide mediated Release of folate-targeted liposome contents from endosomal compartments. *J. Am. Chem. Soc. 118*, 1581–1586.

(48) Rozema, D. B., Ekena, K., Lewis, D. L., Loomis, A. G., and Wolff, J. A. (2003) Endosomolysis by masking of a membrane-active agent (EMMA) for cytoplasmic release of macromolecules. *Bioconjugate Chem. 14*, 51–57.

(49) Morris, M. C., Depollier, J., Mery, J., Heitz, F. C., and Divita, G. (2001) A peptide carrier for the delivery of biologically active protens into mammalian cells. *Nat. Biotechnol. 19*, 1173–1176.

BC700466Z